Available online at www.sciencedirect.com
ScienceDirect
Trans. Nonferrous Met. Soc. China 22(2012) 1995−1999
Transactions of Nonferrous Metals Society of China
www.tnmsc.cn

Phase structure and electrochemical properties of $La_{1.7+x}Mg_{1.3-x}(NiCoMn)_{9.3}$($x$=0−0.4) hydrogen storage alloys

WEI Fan-song[1], LI Li[2], XIANG Hong-fu[1], LI Hui[1], WEI Fan-na[1]

1. School of Materials Science and Engineering, Jiangsu University of Science and Technology, Zhenjiang 212003, China;
2. Environment Monitoring Center of Zhenjiang City, Zhenjiang 212000, China

Received 1 August 2011; accepted 21 December 2011

Abstract: The phase structure and electrochemical properties of $La_{1.7+x}Mg_{1.3-x}(NiCoMn)_{9.3}$($x$=0−0.4) alloys were investigated. The XRD analysis reveals that the alloys consist of $LaNi_5$ phase and other phases, such as $LaMg_2Ni_9$ phase ($PuNi_3$ structure) and La_4MgNi_{19} phases (Ce_5Co_{19}+Pr_5Co_{19} structure, namely A_5B_{19} type). With the increase of the x value, the $LaMg_2Ni_9$ phase fades away and La_4MgNi_{19} phases appear, while the abundance of $LaNi_5$ phase firstly increases and then decreases. At the same time, the cell volume of $LaNi_5$ phase and $LaMg_2Ni_9$ phase decreases. The electrochemical measurement shows that alloy electrodes could be activated in 4−5 cycles, and with the increase of the x value, the maximum discharge capacity gradually increases from 330.9 mA·h/g (x=0) to 366.8 mA·h/g (x=0.4), but the high-rate dischargeability (HRD) and cyclic stability (S) decrease somewhat (x=0.4, HRD_{600}=82.32%, S_{100}=73.8%). It is found that the HRD is mainly controlled by the electrocatalytic activity on the alloy electrode surface, and the decline of cyclic stability is due to the appearance of A_5B_{19} type phase with larger hydrogen storage capacity, which leads to larger volume expansion and more intercrystalline stress and then easier pulverization during charging/discharging.
Key words: hydrogen storage alloy; A_5B_{19} type; crystal structure; electrochemical property; La−Mg−Ni system

1 Introduction

With the development of portable electronic devices and equipments, the demand for Ni/MH battery with higher capacity is ever growing. Mischmetal-based AB_5-type alloys are now widely used as the negative electrode materials for Ni/MH batteries, but their maximum discharge capacity is generally 330 mA·h/g or so which is approaching the theoretical capacity limited by single $CaCu_5$ type structure. It is difficult to meet the demand for increasing energy density of Ni/MH secondary battery [1]. In recent years, a great attention to La−Mg−Ni system alloys has been paid owing to the benefit of low cost and high discharge capacity. KADIR et al [2,3] revealed that RMg_2Ni_9 (R=rare earth, Ca or Y) alloys still held $PuNi_3$-type rhombohedral structure after hydriding, and their hydrogen storage capacity could reach 1.7%−1.8% (mass fraction) through the appropriate element substitution, which was significantly higher than that of the mischmetal-based AB_5-type alloys. Subsequently, CHEN et al [4] found that the discharge capacity of $LaCaMg_2Ni_9$ alloy was up to 360 mA·h/g, but the high-rate dischargeability (HRD) and cyclic stability were poor. KOHNO et al [5] investigated the properties of $AB_{3-3.5}$-type alloy electrode in La−Mg−Ni system, and found that at room temperature, the $La_{0.7}Mg_{0.3}Ni_{2.8}Co_{0.5}$ alloy had a discharge capacity of 410 mA·h/g which increased by 25% compared with the AB_5-type alloy, a better capacity retention rate after 30 cycles and a higher high-rate dischargeability, so it is considered to be a promising candidate for the negative electrode materials for Ni/MH batteries. However, considering the commercial applications, the overall electrochemical properties of such alloys have to be further improved. Researches have indicated that changing the stoichiometry [6,7] and partial substituting the elements of the alloy [8−14] are effective ways to improve the cycle life of alloy, at the same time, the cyclic stability can also be improved significantly by use of different material processing methods such as heat treatment [15,16] and rapid solidification [17,18]. In this work,

Foundation item: Project (2008CL068L) supported by the Natural Science Research Project of Higher Education of Jiangsu Province, China; Project (50901036) supported by the National Natural Science Foundation of China
Corresponding author: WEI Fan-song; Tel: +86-511-85809119; E-mail: zju.wei@yahoo.com.cn
DOI: 10.1016/S1003-6326(11)61419-2

$La_{1.7+x}Mg_{1.3-x}Ni_{7.05}Co_{1.98}Mn_{0.27}$ (x=0−0.4) alloys were prepared by vacuum melting followed with an annealing treatment, and the influence of mass ratio of La to Mg on the phase structure and electrochemical properties of the alloys was investigated in order to improve the overall electrochemical properties of the alloys.

2 Experimental

The alloy samples were prepared by vacuum levitation melting in argon atmosphere and remelted three times to ensure a high homogeneity. The purity of all starting elemental metals was higher than 99.9%. Half the as-cast ingot was annealed under vacuum at 1173 K for 12 h.

The alloy samples thus prepared were ground mechanically into powders below 50 μm and used for electrochemical tests and XRD analysis. The crystal structure of the alloy samples was determined by XRD analysis using a Rigaku D/max 2500/PC diffractometer with Cu K_α radiation, and the XRD patterns were obtained by the step scan mode with step size of 2θ=0.02 °.

For electrochemical tests, pellet type alloy electrodes (d=10mm) were prepared by cold pressing the mixture of the alloy powder with carbonyl Ni powder in a mass ratio of 1:4. The electrochemical tests were carried out at 298 K in a conventional tri-electrode cell consisting of a working electrode (MH electrode), a sintered Ni(OH)/NiOOH counter electrode and a Hg/HgO reference electrode, and the electrolyte was 6 mol/L KOH solution. The discharge capacity was determined galvanostatically by using an automatic charge/discharge unit (Land). Each electrode was charged at 100 mA/g for 4.5 h, and discharged at 60 mA/g to the cut-off potential of −0.7 V (vs Hg/HgO). The high-rate dischargeability (HRD) defined as $C_n/(C_n+C_{60})$ was determined by the ratio of the discharge capacity C_n (with n=300 or 600 mA/g, respectively) to the total discharge capacity defined as the sum of C_n and C_{60}, which was the additional capacity measured subsequently at 60 mA/g after C_n was measured. The cycling test was conducted at the charge/discharge current density of 100 mA/g. The cyclic capacity retention rate S_{100} was defined as $S_{100}=C_{100}/C_{max}$, where C_{100} was the discharge capacities at the 100th cycles. In evaluating the kinetic properties of the electrode reaction, the linear polarization curves of the electrode were plotted with a Solarton SI 1287 potentiostat by scanning the electrode potential at the rate of 0.1 mV/s from −5 to 5 mV(versus open circuit potential) at 50% depth of discharge (DOD). The potentiostatic discharge technique was used to evaluate the diffusion coefficient of hydrogen within the alloy bulk. After being fully charged and followed by a 30 min open circuit rest-period, the test electrodes were discharged with 600 mV potential-step for 2000 s on a Sloartron SI1287 potentiostat, and then the experimental data were analyzed by using the CorrWare electrochemical corrosion software.

3 Results and discussion

3.1 Phase structure

Figure 1 shows the XRD patterns of annealed $La_{1.7+x}Mg_{1.3-x}(NiCoMn)_{9.3}$($x$=0−0.4) alloys. It can be seen that all the alloys are composed of $LaNi_5$ phase ($CaCu_5$ structure, space group: $P6/mmm$) and some other phases, such as $LaMg_2Ni_9$ phase ($PuNi_3$ structure, space group: R-3m) and La_4MgNi_{19} phases with A_5B_{19} type structure (Ce_5Co_{19}+Pr_5Co_{19}, space groups are R-3m and $P6_3/mmc$ respectively). With the increase of the x value, the diffraction peaks of the $LaMg_2Ni_9$ phase become lower, and when x=0.4, the peaks of the $LaMg_2Ni_9$ phase disappear, while those of La_4MgNi_{19} phases appear. This indicates that the reduction of Mg content in the alloy can promote the increase of La_4MgNi_{19} phases.

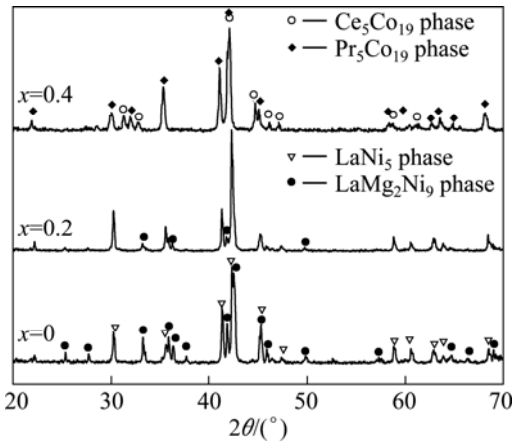

Fig. 1 XRD patterns of annealed $La_{1.7+x}Mg_{1.3-x}(NiCoMn)_{9.3}$ (x=0−0.4) alloys

Figure 2 shows the XRD Rietveld analysis patterns of $La_{2.1}Mg_{0.9}Ni_{7.05}Co_{1.98}Mn_{0.27}$ alloys, in which the fitting factor (R_p) is 11.6 and goodness of fit (S) is 1.9. The fitting results reveal that the Mg occupies the 4f and 6c positions of La atom in A_5B_{19} type structure, with the same occupation as Mg in $PuNi_3$ structure. The phase composition and lattice parameters of the phases in alloys were calculated by the Rietveld method and are listed in Table 1. It can be seen that as x increases, the abundance of $LaMg_2Ni_9$ phase gradually decreases from 61.29% (x=0) to none (x=0.4), but that of $LaNi_5$ phase firstly increases from 38.71% (x=0) to 63.32% (x=0.2) and then decreases to 26.31% (x=0.4). This indicates that

the higher mass ratio of La to Mg easily leads to the transformation of $LaMg_2Ni_9$ phase into $LaNi_5$ phase and further into La_4MgNi_{19} phase (Ce_5Co_{19}+Pr_5Co_{19} type). It can also be seen from Table 1 that the cell volumes of $LaMg_2Ni_9$ phase and $LaNi_5$ phase tend down with the increase of x. For example, the volume of $LaNi_5$ phase decreases from 88.6254×10^{-3} nm^3 (x=0) to 88.4473×10^{-3} nm^3 (x=0.4), which may be due to the phase transformation and the variation of their abundance.

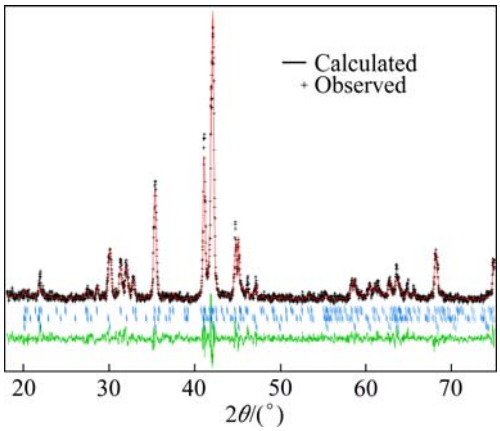

Fig. 2 X-ray diffraction patterns for $La_{2.1}Mg_{0.9}Ni_{7.05}Co_{1.98}Mn_{0.27}$ alloy

3.2 Electrochemical properties

3.2.1 Characteristics of discharge platform

Figure 3 shows the electrochemical plateau curves for hydrogen desorption of $La_{1.7+x}Mg_{1.3-x}(NiCoMn)_{9.3}$ (x=0−0.4) alloys. As can be seen from Fig.3, although all the alloys are composed of double phases or multiphases, their discharging plateau curves show a characteristics of single platform, which may be ascribed to their

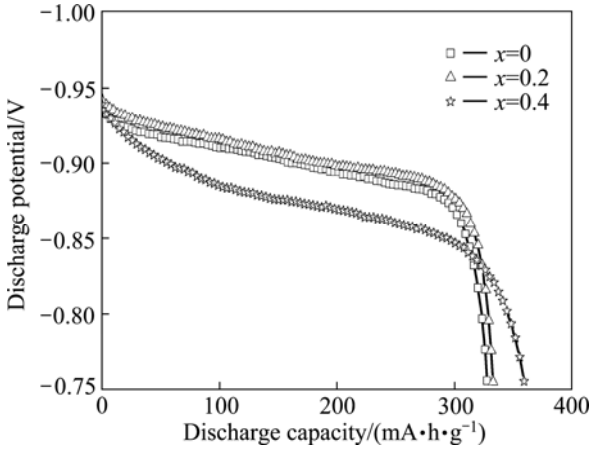

Fig. 3 Electrochemical plateau curves for hydrogen desorption of $La_{1.7+x}Mg_{1.3-x}(NiCoMn)_{9.3}$ (x=0−0.4) alloys at 298 K

approximate plateau pressures. When x=0.4, the plateau lowers obviously, and referring to the Rietveld analysis in Table 1, the total mass fraction of La_4MgNi_{19} phase (Ce_5Co_{19}+Pr_5Co_{19} type structure) with larger cell volume is up to 73.69%, which adds the hydrogen position in the alloy and then leads to a lower platform and a higher capacity.

3.2.2 Activation performance and discharge capacity

The electrochemical properties of the alloys are summarized in Table 2. It can be seen that alloy electrodes can be activated in 4−5 cycles, and with x increasing, the maximum discharge capacity gradually increases from 330.9 mA·h/g (x=0) to 366.8 mA·h/g (x=0.4). This means that the higher mass ratio of La to Mg has a little influence on the activation performance, but can significantly enhance the original capacity, which may be related to the higher hydrogen storage capacity of La_4MgNi_{19} phases (about 1.5%).

Table 1 Phase composition and lattice parameters of $La_{1.7+x}Mg_{1.3-x}(NiCoMn)_{9.3}$ (x=0−0.4) alloys

x	Phase	Space group	Phase abundance/%	Lattice constant		Cell volume, V/10^{-3} nm^3
				a/nm	c/nm	
0	$LaMg_2Ni_9$	$R\bar{3}m$ (166)	61.29	0.50119	2.41186	524.6725
	$LaNi_5$	$P6/mmm$ (191)	38.71	0.50521	0.40095	88.6254
0.2	$LaMg_2Ni_9$	$R\bar{3}m$ (166)	36.68	0.50106	2.41225	524.4912
	$LaNi_5$	$P6/mmm$ (191)	63.32	0.50502	0.40085	88.5375
0.4	Ce_5Co_{19}	$R\bar{3}m$ (166)	46.21	0.50567	4.84638	1073.2166
	Pr_5Co_{19}	$P6_3/mmc$ (194)	27.48	0.50643	3.22818	717.0241
	$LaNi_5$	$P6/mmm$ (191)	26.31	0.50501	0.40048	88.4473

Table 2 Electrochemical properties of $La_{1.7+x}Mg_{1.3-x}(NiCoMn)_{9.3}$ (x=0−0.4) alloys

x	C_{max}/(mA·h·g^{-1})	n	HRD_{300}/%	HRD_{600}/%	J_0/(mA·g^{-1})	D/(10^{-10} cm^2·s^{-1})	S_{100}/%
0	330.9	5	97.17	93.01	122.3	3.01	83.9
0.2	337.2	4	97.66	93.43	128.5	2.89	80.1
0.4	366.8	4	92.69	82.32	105.1	2.51	73.8

n: Cycle number

3.2.3 High-rate dischargeability

From Table 2, it is also found that the high-rate dischargeabilities of alloys at x=0 and x=0.2 are similar, and when the x value further increases to 0.4, the HRD decreases obviously. At the discharge rate of 300 mA/g, the HRD_{300} of x=0 or x=0.2 alloy is around 97%, but that of x=0.4 alloy is only 92.69%. When the discharge current increases to 600 mA/g, the HRD_{600} of x=0 or x=0.2 alloy is up to 93%, but that of x=0.4 alloy obviously decreases to 82.32%. It is known that the high-rate dischargeability of MH electrode is mainly influenced by the electrochemical reaction rate on the alloy surface and the diffusion rate of hydrogen in the bulk of the alloy [19]. To examine the factors of discharge kinetics in alloy electrodes, linear polarization and potential-step experiment were performed on the alloy electrodes, and then exchange current density (J_0) and hydrogen diffusion coefficient (D) were calculated respectively according to the obtained curves, as listed in Table 2, and the detailed calculating method can be seen in Ref. [20]. As shown in Table 2, with the increase of the x value, the exchange current density (J_0) of alloy electrodes firstly increases and then decreases, but the hydrogen diffusion coefficient (D) continuously decreases from 3.01×10^{-10} cm^2/s (x=0) to 2.51×10^{-10} cm^2/s (x=0.4). Comparing the HRD with the values of J_0 and D, it is found that the variation of J_0 is consistent with that of HRD values of the alloy electrodes. This indicates that the HRD is mainly controlled by the electrocatalytic activity on the alloy electrode surface.

3.2.4 Cyclic stability

Figure 4 shows the cyclic stability curves of alloy electrodes. From Table 2 and Fig. 4, it can be seen that the alloy with higher x value shows further poor cycling stability. For x=0.4 alloy, although its cycling stability declines obviously, the capacity retention rate (S_{100}) of the alloy after 100 cycles is still up to 73.8%. As seen from the above analysis, there are Ce_5Co_{19}+Pr_5Co_{19} type phases with larger hydrogen storage capacity for x=0.4 alloy, which causes larger cell volume expansion and more intercrystalline stress, then resulting in easier pulverization during charge/discharge. It is well accepted that a higher degree of pulverization exposes more surface area to the corrosive electrolyte, then corrodes more and hence has a poor cycling stability.

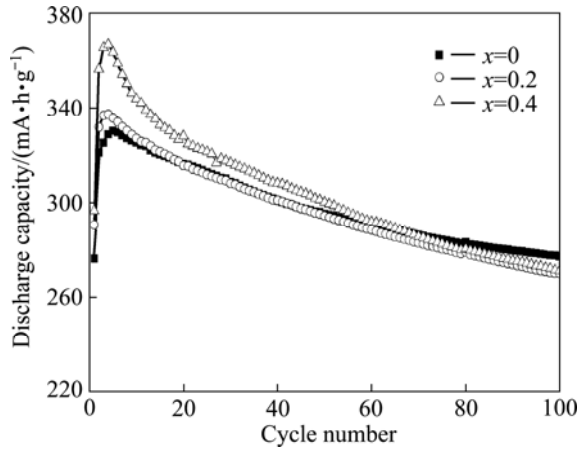

Fig. 4 Cyclic stability curves of alloy electrodes at 298 K

4 Conclusions

1) The structure analysis reveals that all the alloys are composed of $LaNi_5$ phase ($CaCu_5$ structure) and other phases, such as $LaMg_2Ni_9$ phase ($PuNi_3$ structure) and La_4MgNi_{19} phases with A_5B_{19} type structure (Ce_5Co_{19}+Pr_5Co_{19}). With the increase of the x value, the $LaMg_2Ni_9$ phase disappears and La_4MgNi_{19} phase appears, but the abundance of $LaNi_5$ phase increases firstly and then decreases. At the same time, the cell volume of $LaNi_5$ and $LaMg_2Ni_9$ decreases.

2) The electrochemical measurement shows that the increase of x value improves the activation and initial capacity, but lowers the high-rate dischargeability somewhat. It is found that the HRD is mainly controlled by the electrocatalytic activity on the alloy electrode surface, and the decline of cyclic stability is due to the appearance of A_5B_{19} type phase with larger hydrogen storage capacity, which leads to larger volume expansion and intercrystalline stress and then easier pulverization during charge/discharge.

3) $La_{2.1}Mg_{0.9}(NiCoMn)_{9.3}$ alloy shows a high capacity (366.8 mA·h/g), reasonable cyclic stability (S_{100}=73.8%) and good 1 C rate dischargeability (HRD_{300}= 92.69%), which is a promising candidate for a high capacity negative electrode material for Ni/MH batteries.

References

[1] LEI Yong-quan. New energy materials [M]. Tianjin: Tianjin University Press, 2000: 44−45. (in Chinese)

[2] KADIR K, SAKAI T, UEHARA I. Structural investigation and hydrogen capacity of YMg_2Ni_9 and $(Y_{0.5}Ca_{0.5})(MgCa)Ni_9$: New phases in the AB_2C_9 system isostructural with $LaMg_2Ni_9$ [J]. J Alloys Comp, 1999, 287: 264−270.

[3] KADIR K, SAKAI T, UEHARA I. Structural investigation and hydrogen storage capacity of $LaMg_2Ni_9$ and $(La_{0.65}Ca_{0.35})(Mg_{1.32}Ca_{0.68})Ni_9$ of the AB_2C_9 type structure [J]. J Alloys Comp, 2000, 302: 112−117.

[4] CHEN J, KURIYAMA N, TAKESHITA H T, TANAKA H, SAKA T, HARUTA M. Hydrogen storage alloys with $PuNi_3$-type structure as metal hydride electrodes [J]. Electrochem Solid-State Lett, 2000, 3(6): 249−252.

[5] KOHNO T, YOSHIDA H, KAWASHIMA F, INDABA T, SAKAI I, YAMAMOTO M, KANDA M. Hydrogen storage properties of new ternary system alloys: La_2MgNi_9, $La_5Mg_2Ni_{23}$, La_3MgNi_{14} [J]. J Alloys Comp, 2000, 311: L5−L7.

[6] PAN H G, LIU Y F, GAO M X, LEI Y Q, WANG Q D. Study of the structural and electrochemical properties of $La_{0.7}Mg_{0.3}(NI_{0.85}Co_{0.15})_x$

(x=2.5−5.0) hydrogen storage alloys [J]. J Electrochem Soc A, 2003, 150: 565−570.

[7] LIU Y F, PAN H G, GAO M X, LI R, LEI Y Q. Influence of Ni addition on the structures and electrochemical properties of $La_{0.7}Mg_{0.3}Ni_{2.65+x}Co_{0.75}Mn_{0.1}$ (x=0−0.5) hydrogen storage alloys [J]. J Alloys Comp, 2005, 389(1−2): 281−289.

[8] LIAO B, LEI Y Q, CHEN L X, LU G L, PAN H G, WANG Q D. Effect of the La/Mg ratio on the structure and electrochemical properties of $La_xMg_{3-x}Ni_9$ (x=1.6−2.2) hydrogen storage electrode alloys for nickel-metal hydride batteries [J]. J Power Source, 2004, 129: 358−367.

[9] TANG Rui, LIU Li-qin, LIU Yong-ning, YU Guang, ZHU Jie-wu, LIU Xiao-dong. Structure and electrochemical properties of $La_{0.8-x}RE_xMg_{0.2}Ni_{3.2}Co_{0.6}$ hydrogen storage alloys [J]. The Chinese Journal of Nonferrous Metals, 2005, 15(7): 1057−1061. (in Chinese)

[10] LIAO Bin, LEI Yong-quan, CHEN Li-xin, LÜ Guang-lie, PAN Hong-ge, WANG Qi-dong. A study on the structure and electrochemical properties of $La_2Mg(Ni_{0.95}M_{0.05})_9$ (M=Co, Mn, Fe, Al, Cu, Sn) hydrogen storage electrode alloys[J]. Journal of Alloys and Compounds, 2004, 376(1−2): 186−195.

[11] ZHANG X B, SUN D Z, YIN W Y, CHAI Y J, ZHAO M S. Crystallographic and electrochemical characteristics of $La_{0.7}Mg_{0.3}Ni_{3.5-x}(Al_{0.5}Mo_{0.5})_x$ (x=0−0.8) hydrogen storage alloys [J]. J Power Sources, 2006, 154: 290−297.

[12] ZHANG Fa-liang, LUO Yong-chun, SUN Kai, KANG Long, CHEN Jian-hong. A study on the structure and electrochemical properties of $La_{1.5}Mg_{0.5}Ni_{7-x}Co_x$ (x=0−1.8) hydrogen storage alloys [J]. Functional Materials, 2006, 37(2): 265−268. (in Chinese)

[13] LIU Y F, PAN H G, GAO M X, ZHU Y F, LEI Y Q, WANG Q D. Structures and electrochemical properties of $La_{0.7}Mg_{0.3}Ni_{2.975-x}Co_{0.}525Mnx$ hydrogen storage alloys [J]. J Electrochem Soc A, 2004, 151(3): 374−380.

[14] JIANG Bing-jie, WANG Jing, MU Dao-bin, CHEN Shi, WU Bo-rong, WU Feng. Effect of Al substitution on electrochemical performance of La−Mg−Ni hydrogen storage alloys [J]. The Chinese Journal of Nonferrous Metals, 2008, 18(11): 2036−2043. (in Chinese)

[15] LIU Y F, PAN H G, GAO M X, ZHU Y F, LEI Y Q. Influence of heat treatment on electrochemical characteristics of $La_{0.}75Mg0_{.25}Ni_{2.8}Co_{0.5}$ hydrogen storage electrode alloy [J]. Transactions of Nonferrous Metals Society of China, 2003, 13: 25−28.

[16] ZHOU Zeng-lin, SONG Yue-qing, CUI Shun, LIN Chen-guang, GUO Zhi-meng, QU Xuan-hui. Effect of heat treatment on the properties of La−Mg−Ni-system hydrogen storage electrode alloys (II) Hydrogen storage and electrochemical properties [J]. Rare Metal Materials and Engineering, 2008, 37(6): 964−969. (in Chinese)

[17] ZHANG Yang-huan, DONG Xiao-ping, WANG Guo-qing, GUO Shi-hai, REN Jiang-yuan, WANG Xin-lin. Cycling stability of La−Mg−Ni system ($PuNi_3$-type) hydrogen storage alloys prepared by casting and rapid quenching [J]. The Chinese Journal of Nonferrous Metals, 2005, 15(5): 705−710. (in Chinese)

[18] ZHANG Yang-huan, ZHAO Dong-liang, DONG Xiao-ping, QI Yan, GUO Shi-hai, WANG Xin-lin. Effects of rapid quenching on structure and electrochemical characteristics of $La_{0.5}Ce_{0.2}Mg_{0.3}Co_{0.4}Ni_{2.6-x}Mn_x$ (x=0−0.4) electrode alloys [J]. Transactions of Nonferrous Metals Society of China, 2009, 19(2): 364−371.

[19] IWAKURA C, OURA T, INOUSE H, MASTSUOKA M. Effects of substitution with foreign metals on the crystallographic, thermodynamic and electrochemical properties of AB_5-type hydrogen storage alloys [J]. Electrochim Acta, 1996, 41(1): 117−121.

[20] WEI Fan-song, LEI Yong-quan, CHEN Li-xin, YING Tiao, GE Hong-wei, LÜ Guang-lie. Influence of material processing on crystallographic and electrochemical properties of cobalt-free $LaNi_{4.95}Sn_{0.3}$ hydrogen storage alloy [J]. Transactions of Nonferrous Metals Society of China, 2006, 16(3): 527−531.

$La_{1.7+x}Mg_{1.3-x}(NiCoMn)_{9.3}$($x$=0~0.4)贮氢合金的相结构与电化学性能

魏范松[1]，黎　莉[2]，项宏福[1]，李　惠[1]，魏范娜[1]

1. 江苏科技大学 材料科学与工程学院，镇江 212003；
2. 江苏省镇江市环境监测中心站，镇江 212000

摘　要：对 $La_{1.7+x}Mg_{1.3-x}(NiCoMn)_{9.3}$($x$=0~0.4)贮氢合金相结构和电化学性能进行研究。结构分析表明，合金主要由 $LaNi_5$ 相($CaCu_5$ 结构)和其他相组成，如 $LaMg_2Ni_9$ 相 ($PuNi_3$ 结构) 或 La_4MgNi_{19} 相(Ce_5Co_{19}+Pr_5Co_{19} 结构)。随着 x 的增加，$LaMg_2Ni_9$ 相消失并出现 La_4MgNi_{19} 相，而 $LaNi_5$ 相的含量则先增加后减小，且晶胞体积下降。电化学分析表明，合金电极只需 4、5 次循环即可活化；随着 x 的增加，最大放电容量逐渐增大，从 x=0 的 330.9 mA·h/g 增加到 x=0.4 的 366.8 mA·h/g，但高倍率放电性能(HRD)和循环稳定性(S)则有所下降(x=0.4, HRD_{600}=82.32%, S_{100}=73.8%)。研究认为，HRD 主要由合金电极表面的电催化活性控制，而循环稳定性的下降则是由于 x=0.4 合金中出现了具有较大吸氢量的 Ce_5Co_{19} 和 Pr_5Co_{19} 型结构相，导致吸氢膨胀率和晶间应力增大，使合金颗粒在吸放氢过程中较易粉化所致。

关键词：贮氢合金；A_5B_{19} 型；晶体结构；电化学性能；La−Mg−Ni 系

(Edited by LI Xiang-qun)